



A simplified qPCR method revealing tRNAome remodeling upon infection by genotype 3 hepatitis E virus

Xumin Ou^{1,2} , Buyun Ma², Ruyi Zhang², Zhijiang Miao², Anchun Cheng^{1,3,4}, Maikel P. Peppelenbosch²  and Qiuwei Pan²

1 Institute of Preventive Veterinary Medicine, Sichuan Agricultural University, Chengdu, China

2 Department of Gastroenterology and Hepatology, Erasmus MC – University Medical Center Rotterdam, The Netherlands

3 Key Laboratory of Animal Disease and Human Health of Sichuan Province, Sichuan Agricultural University, Chengdu, China

4 Research Center of Avian Diseases, College of Veterinary Medicine, Sichuan Agricultural University, Chengdu, China

Correspondence

Q. Pan, Department of Gastroenterology and Hepatology, Erasmus MC – University Medical Center Rotterdam, Room Na-1005, PO Box 2040, NL-3000 CA Rotterdam, The Netherlands

Tel: +31 107 037502

E-mail: q.pan@erasmusmc.nl

and

A. Cheng, Institute of Preventive Veterinary Medicine, Sichuan Agricultural University, Chengdu, Sichuan 611130, China

Tel: +86 133 08165183

E-mail: chenganchun@vip.163.com

Xumin Ou, Buyun Ma, and Ruyi Zhang contributed equally to this work

(Received 10 January 2020, revised 8 February 2020, accepted 21 February 2020)

doi:10.1002/1873-3468.13764

Edited by Michael Ibba

The landscape of tRNA–viral codons regulates viral adaption at the translational level, presumably through adapting to host codon usage or modulating the host tRNAome. We found that the major zoonotic genotype of hepatitis E virus (HEV) has not adapted to host codon usage, prompting exploration of the effects of HEV infection on the host tRNAome. However, tRNAome quantification is largely impeded by the extremely short sequences of tRNAs and redundancy of tRNA genes. Here, we present a length-extension and stepwise simplified qPCR method that utilizes a universal DNA/RNA hybrid tRNA adaptor and degenerate primers. Using this novel methodology, we observe that HEV infection dramatically reprograms the hepatic tRNAome, which is likely to facilitate translation of viral RNAs. This tRNAome quantification method bears broad implications for future tRNA research and possibly tRNA-based diagnostics.

Keywords: hepatitis E virus; length-extension and simplified qPCR method; tRNAome

Viral adaption is shaped by a variety of effectors, including the need to hijack the cellular protein-synthesizing machinery for efficient translation of viral genes [1]. Rate-limiting steps in the production of viral proteins differ depending on host species and the virus involved. But in many cell types, the efficiency of the translational machinery is critically dependent on tRNA availability for decoding both cellular and viral codons [2,3]. Accordingly, many viruses show adaptation with respect to codon usage toward their host [4–7].

Conversely, it has been reported that interferons, the potent antiviral cytokines [8], can alter the availability of tRNAs to facilitate the production of antiviral proteins and to attenuate decoding of viral codons [9,10]. Thus, studying the interplay between viral codons and cellular tRNAome is essential for understanding the infection biology.

tRNAs are the recognition modules that decode the mRNA in the ribosome and are covalently charged by amino acids [11]. Following recognition, the

Abbreviations

CAI, codon adaption index; HEV, hepatitis E virus; ISGs, interferon-stimulated genes; ORF, open reading frame; RSCU, relative synonymous codon usage.

corresponding intramolecular bond is hydrolyzed and the released amino acid is covalently linked to the nascent peptide chain. The tRNAs encoded in genomic DNA are typically 70–90 base pairs in length often with multiple genomic copies of the same tRNA [12]. The human tRNA^{ome} is encoded by more than 600 tRNA gene loci [12]. Following transcription, tRNAs are subjected to post-transcriptional modification, and a common CCA ribonucleotide sequence is added to the 3' end of tRNA [13]. Accurate detection of the mature tRNA^{ome} is technically challenging and especially hampered by the short-length and redundant tRNA genes [14,15]. As the number of different tRNA sequences is relatively limited, we believe that optimized qPCR-based techniques hold possibility for quantifying tRNAs.

Hepatitis E virus (HEV) is a ssRNA(+) virus and is the leading cause of acute viral hepatitis [16]. Globally, HEV causes annually 20 million infections with over 56 000 lethal cases and especially in pregnant women [17]. Among the major genotypes, genotype 1 and 2 HEVs only infect humans, whereas genotypes 3 and 4 are zoonotic. Genotype 3 is highly prevalent in Western countries with a broad host spectrum [18,19]. In this study, we aim to first develop a simplified qPCR method for quantifying mature tRNAs, and then to investigate how codon usage of the zoonotic HEV genotype relates to the human tRNA^{ome} composition.

Materials and methods

Experimental models

For HEV infectious model, a full-length genotype 3 HEV genome (Kernow-C1 p6 clone; GenBank accession number: JQ679013) was used [20]. The human hepatoma Huh7 cell line was used to harbor the HEV genome and produce infectious virus particles for secondary infection of naïve Huh7 cells [21]. The HEV subgenomic model was based on Huh7 cells containing the subgenomic genotype 3 HEV sequence (Kernow-C1 p6/luc) coupled to a *Gaussia* luciferase reporter gene [21,22]. The cell line was regularly checked for identity using STR verification as provided by the pathology department of the Erasmus MC. Key reagents, viral strains, and software used in this study are listed in Table S1.

Bioinformatic analysis

Codon usage bias and codon adaptation index (CAI) of HEV ORF (1–3) and interferon-stimulated genes (ISGs) were analyzed by CODONW software (<http://www.molbiol.ox.ac.uk/cu>, version 1.4.2) using standard genetic codes. Correlation analysis was performed by PYTHON MATPLOTT package (<https://matplotlib.org>). Codon usage and tRNA^{ome} data were

visualized by HEMI software with hierarchical clustering analysis (<http://hemi.biocuckoo.org/>).

The qPCR protocol for quantifying mature tRNAs

Preparation of samples and reagents – Timing 1 day

1 Prepare primary cells, cell lines, or tissues to yield 1–4 μg total RNA for each sample. This amounts to roughly 10^5 – 10^6 mammalian cells. These values are rough guidelines for experimental design, but yields will vary according to the cell types and amounts.

(Optional) Protocol can begin with isolated RNA samples. In this case, we recommend to adjust RNA concentration to $214 \text{ ng}\cdot\mu\text{L}^{-1}$. Then, mix $4 \mu\text{L}$ RNA sample with $1 \mu\text{L}$ $5\times$ deacylation buffer (step 9) and incubate at 37°C for 40 min; after that, add $10 \mu\text{L}$ TE buffer for PH adjustment (step 10). Finally, $7 \mu\text{L}$ of the RNA containing deacylated tRNAs ($400 \text{ ng} \approx 214 \text{ ng}\cdot\mu\text{L}^{-1} \times 4/15 \times 7 \mu\text{L}$) is ready for the following annealing with U-adaptor (step 11).

Total RNA isolation and tRNA deacylation – Timing 1.5–2 h

- 2 Wash cells. Remove cell medium and wash cells with warm PBS buffer.
- 3 Lyse cells. Add $350 \mu\text{L}$ of RA lysis buffer to each well, then suck up whole-cell lysate into 1.5 mL EP tube. All the reagents for RNA extraction except deacylation buffer are provided by NucleoSpin[®] RNA kit.
- 4 Adjust RNA binding condition. Add $350 \mu\text{L}$ 70% ethanol to the homogenized lysate and mix by pipetting up and down (minimal five times).
- 5 RNA binding. For each sample, take one NucleoSpin[®] RNA Column and place in a collection tube. Pipette lysate up and down 2–3 times and load the lysate to the column. Centrifuge for 30 s at $11\ 000 \text{ g}$. Place the column on a new collection tube (2 mL).
- 6 Desalt silica membrane. Add $350 \mu\text{L}$ MDB (Membrane Desalting Buffer) and centrifuge at $11\ 000 \text{ g}$ for 1 min to dry the membranes.
- 7 Digest DNA. Prepare DNase reaction mixture in a sterile 1.5 mL tube. For each isolation, add $10 \mu\text{L}$ DNase to $90 \mu\text{L}$ reaction buffer for DNase. Mix by flicking the tube. Add $95 \mu\text{L}$ DNase reaction mixture directly onto the center of the silica membrane of the column. Incubate at room temperature for 15 min.
- 8 Wash and dry the silica membrane.

1st Wash: Add $200 \mu\text{L}$ RAW2 buffer to the NucleoSpin[®] RNA Column. Centrifuge for 30 s at $11\ 000 \text{ g}$. Place the column on a new collection tube (2 mL).

2nd Wash: Add $600 \mu\text{L}$ RA3 buffer to the NucleoSpin[®] RNA Column. Centrifuge for 30 s at $11\ 000 \text{ g}$. Place the column on a new collection tube (2 mL).

3rd Wash: Add 250 μ L RA3 buffer to the NucleoSpin[®] RNA Column. Centrifuge for 2 min at 11 000 *g* to dry the membrane completely. Place the column on a new collection tube (2 mL).

- 9 Deacylation. Prepare deacylation mixture. Add 2 μ L of 5 \times Tris/HCl (100 mM PH 9.0) into 8 μ L ddH₂O; mix it by pipetting up and down (minimal five times). Add 10 μ L Deacylation mixture to the NucleoSpin[®] RNA Column. Incubate at 37 $^{\circ}$ C for 40 min.
- 10 Elute RNA. Place the column on a new 1.5 mL EP tube. Elute the RNA by adding an additional 20 μ L TE buffer on the NucleoSpin[®] RNA Column directly. Centrifuge for 1 min at 11 000 *g*.

Adaptor ligation – Timing 1.5–2 h

- 11 Annealing and measuring RNA concentration by Nano-Drop. Prepare mixture of 400 ng RNA and 20 pm adaptor (2 μ L); then, the final volume is adjusted to 9 μ L. Incubate at 90 $^{\circ}$ C for 3 min.
- 12 Add 1 μ L 10 \times Tris/HCl (50 mM, pH 8.0) annealing buffer at 37 $^{\circ}$ C for 20 min.
- 13 Ligation reaction. Add 2 μ L ligase buffer, 7.9 μ L H₂O, and 0.1 μ L T4 RNA ligase into the above mixture, then incubate at 37 $^{\circ}$ C for 1 h.

Reverse transcription – Timing 0.5 h

- 14 Annealing with mixture of specific tRNA reverse primers. Twenty microlitre of the above mixture is added with 3.42 μ L (1.14 μ L \times 3 = 3.42 μ L) of mixture of tRNA reverse primers (Table S2). Incubate the mixture at 65 $^{\circ}$ C for 5 min. Place on ice immediately.
- 15 Coreverse transcript with random and oligo (dT) primers. Add 6 μ L 5 \times PrimeScript RT Master Mix and 0.58 μ L H₂O into the above tube. Mix by flicking the tube. Incubate the mixture at 37 $^{\circ}$ C for 15 min followed by 85 $^{\circ}$ C for 5 s.

qPCR – Timing 1–2 h

- 16 qPCR mix preparation (Table S3). Prepare qPCR mixture according to the following recipe (10 μ L). To cover all 57 tRNA types, we recommend adding 220 μ L ddH₂O into above 30 μ L of reverse transcription solution.

Notice: Because of the large number of tRNA sets, it is recommended to prepare tRNA-X-R and tRNA-X-F primer mixture to minimize loading variation. For example, to prepare 80 times of tRNA-R/F mix, we recommend that

20 μ L (10 pm) of tRNA-X-R and tRNA-X-F was diluted by 200 μ L ddH₂O. Therefore, the finally used volume of tRNA primers mix is 3 μ L.

- 17 Perform qPCR with the designed cycling condition according to Table S4.

Quantification

The $2^{-\Delta\Delta C_t}$ was used to calculate the relative expression of each tRNA species, and the ΔC_t values were determined by subtracting the average C_t values of the endogenous control gene *GAPDH* from the average C_t values of each tRNA type.

Statistical analysis

Linear correlations between the relative synonymous codon usage (RSCU) of human and animal HEV strains were estimated by the Pearson coefficients. Statistical comparisons of tRNA^{ome} data were performed with the Mann–Whitney *U*-test for nonpaired independent samples. $*P \leq 0.05$ was indicated as significant. The statistical analysis was performed using the spss 19.0 software (IBM Corporation, Armonk, NY, USA).

Results

The codon usage of genotype 3 HEV has not adapted to its human host

As in many biological systems, tRNA availability [23] and codon context [24] constitute the rate-limiting step for protein synthesis. Viruses are expected to adapt codon usage to fit host codon usage patterns. With respect to the zoonotic genotype 3 HEV, however, this has not yet been analyzed. Hence, we compared the RSCU of three open reading frames (ORFs) of genotype 3 HEV isolated from human to the counterpart of the human host. Similar analysis was also performed for HEV strains isolated from animals, including swine, deer, mongoose, and wild boar (Table 1). Strikingly, we did not find evidence that the codon usage of genotype 3 HEV isolated from human and the animal host has adapted to the human codon usage pattern for any of the three ORFs investigated (Fig. 1), because linear correlations between the RSCU of human and animal HEV strains are very poor (Pearson coefficients less than 0.40). Moreover, the RSCU analysis of HEV between the nonhuman primate (e.g., monkey) and humans also indicated that the usage of major codons is similar except serine codon (UCU) (Fig. S1). Besides RSCU, the CAI has also been suggested to predict the efficiency of

Table 1. List of HEV genotype 3 strains used in this study

Host	Source material	Country of origin	Collection data	Accession no.
<i>Homo sapiens</i>	Hepatocytes	United Kingdom	July 2010	JQ679013
<i>Sus domesticus</i>	Serum	United States	1997	AF082843
<i>Sus scrofa</i>	Liver	Germany	2006	FJ705359
<i>Cervus nippon</i>	Liver or serum	Japan	22 February 2003	AB189071
<i>Herpestes javanicus</i>	Serum	Japan	2002	AB236320
<i>Cynomolgus</i>	Serum	Japan	November 2009	JQ026407.1

translation elongation [25]. Our results indicated that the CAI of HEV was similar among different host species-derived strains, and much lower than that of human housekeeping gene (e.g., GAPDH) (Fig. 1). We conclude that there has been very little evolutionary pressure on genotype 3 HEV to adapt to the codon usage of its human host. Thus, we decided to investigate how HEV infection regulates the host tRNA^{ome}.

A simplified qPCR method for characterizing the human mature tRNA^{ome}

To develop a novel qPCR method for easy quantification of mature tRNAs, we first designed a DNA/RNA hybrid adaptor (universal adaptor, U-adaptor). It is compatible with all types of mature tRNAs with a common 3' CCA acceptor (Fig. 2). Following binding of the adaptor to the tRNA molecule, the adaptor can be ligated to both the 5' end and 3' end of the mature tRNAs. Of note, the mature tRNAs are frequently charged by amino acids that hamper the above ligation reaction. Thus, a deaminoacylation reaction for the charged tRNA is needed during RNA isolation (see [Materials and methods](#)). Importantly, the adaptor is designed to form a loop and hybridize on tRNA itself. This hybridization is compatible with any type of base pairs adjacent to 3' CCA tail of tRNAs, as the pairing base of the U-adaptor involved is degenerately designed. The ligation reaction specifically links the 5' end and 3' end of the adaptor to the corresponding ends of tRNA molecule that is catalyzed by T4 RNA ligase (Fig. 2). Finally, a hybrid pseudocircular molecule, containing the deaminoacylated original mature tRNA molecule and the U-adaptor, is formed. This strategy serves two important ends: It extends the length of tRNA for subsequent qPCR while simultaneously eliminating immature tRNAs. Afterward, tRNAs can be determined by conventional qPCR (see the experimental strategy and Fig. 3).

To this end, a mixture of tRNA-specific reverse primers was used, with the primers designed to bind to the region between the anticodon loop and the D

loop. A complication with regard to designing reverse primers for characterizing the tRNA^{ome} is that many iso-decoder tRNAs (i.e., tRNA with the same anticodon but vary in backbone) are responsible for decoding of the identical genetic codon [12]. We thus retrieved all 57-human genomic tRNA genes from the GtRNA 2.0 database and accordingly designed degenerate primers (Table S2). Using RNA obtained from Huh7 human liver cells, all primer pairs successfully amplified their iso-decoder tRNA molecules in qPCR (Figs S2 and S3). We conclude that our approach employing the U-adaptor and degenerate primers allows easy quantification of cellular tRNA profiles.

Normalization of tRNA^{ome} by reference gene

In order to normalize tRNA level, tRNA-specific reverse primers, and random and oligo (dT) primers were concurrently used for reverse transcription reaction. GAPDH, a commonly accepted reference gene, is selected for tRNA^{ome} normalization [26]. tRNA-His-GUG is the only tRNA species capable of decoding histidine codons (CAC and CAU), and thus, we expect that its expression would be more stable. Indeed, we observed good correlation between levels of GAPDH mRNA and tRNA-His-GUG (Fig. S4). Comparing the U-adaptor and tRNA-histidine adaptor for ligation reaction, we found that the U-adaptor did not compromise the ligation efficiency as it caused only 0.11 variation calculated by ΔC_t (Table S1). Efforts were made for further optimization of the protocol, for instance, by combining steps including annealing, but these efforts failed (Fig. S5). The final protocol (refer to [Materials and methods](#)) is organized in seventeen discrete steps and allows quantitative assessment of mature tRNA^{ome}.

HEV infection provokes remodeling of the mature tRNA^{ome} in host cells

Although viruses are considered to adapt their codon usage to that of their host [3,27], we observe that HEV

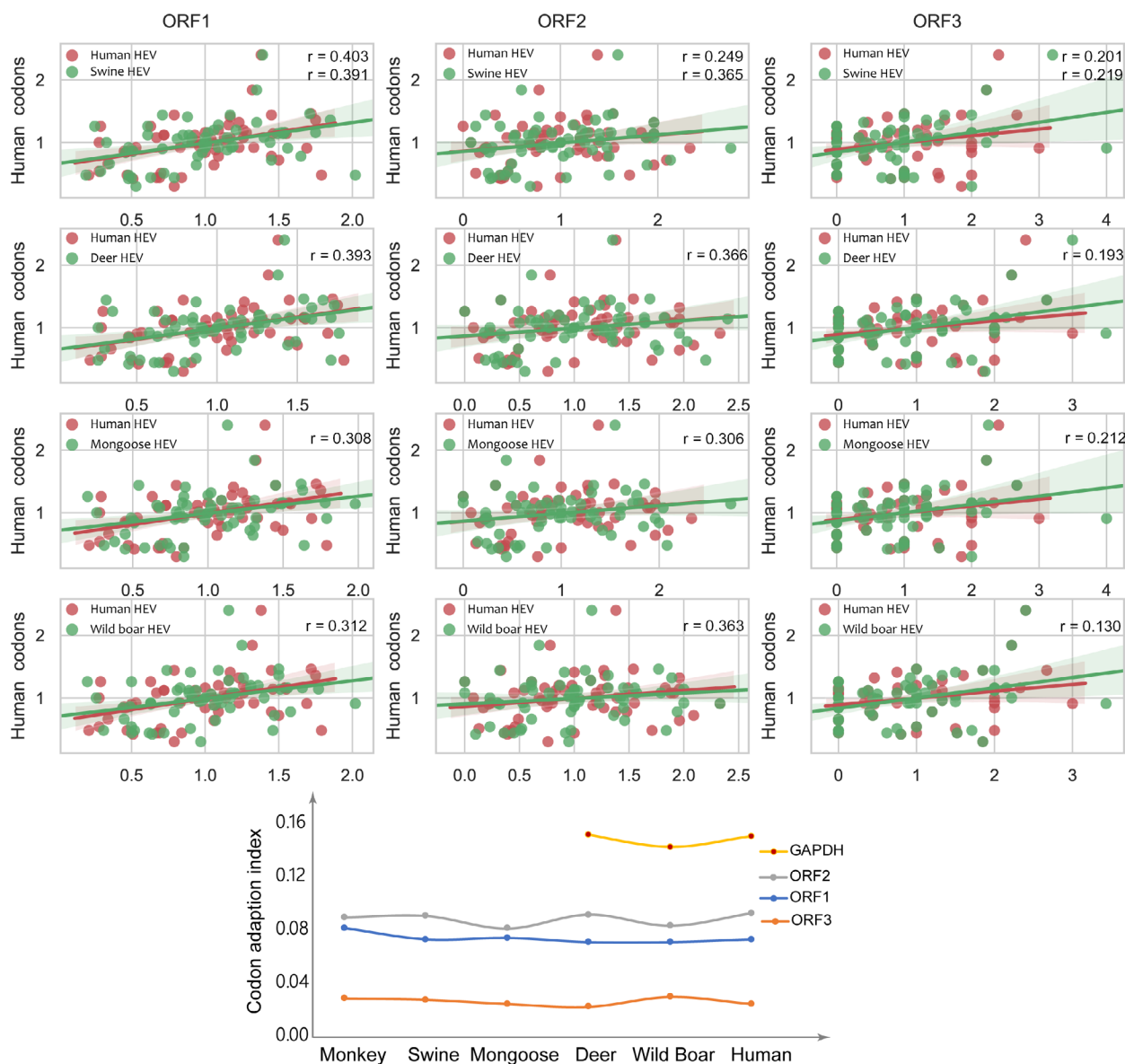


Fig. 1. Lack of adaptation of genotype 3 HEV codon usage to host codon usage. Codon usage of human HEV was correlated with overall human codon usage. The codon usage of swine, wild deer, mongoose, and wild boar HEV was also related to human codon usage. For each possible codon and 64 in total, its RSCU in the human genome is plotted against the y-axis and the corresponding RSCU in the relevant viral ORF on the x-axis. Results were shown for all three ORFs in the upper panels. In the lower panel, CAI of genotype 3 HEV isolated from different host species was compared for ORF1-3. The CAI of GAPDH from deer, wild boar, and humans is also indicated. The CAI calculation was performed by *codonW* software with *Saccharomyces cerevisiae* as reference set.

is not subject to such adaptation. Hence, we decided to compare tRNAome composition in the presence and absence of HEV infection. To this end, Huh7 cells were infected with full-length HEV or exposed to vehicle control (Fig. S4A), and the levels of different tRNAs were determined (Fig. S6A). We observed a major effect on tRNAome remodeling by HEV

infection. A total of 29 of 57 tRNA species showed significant upregulation. The most marked example is tRNA-Pro-GGG that shows 162 times higher expression in HEV-infected cells as compared to noninfected cells. tRNA-Gly-CCC and tRNA-Pro-UGG were approximately 50 times and about 35 times upregulated in HEV-infected cells, respectively. Conversely,

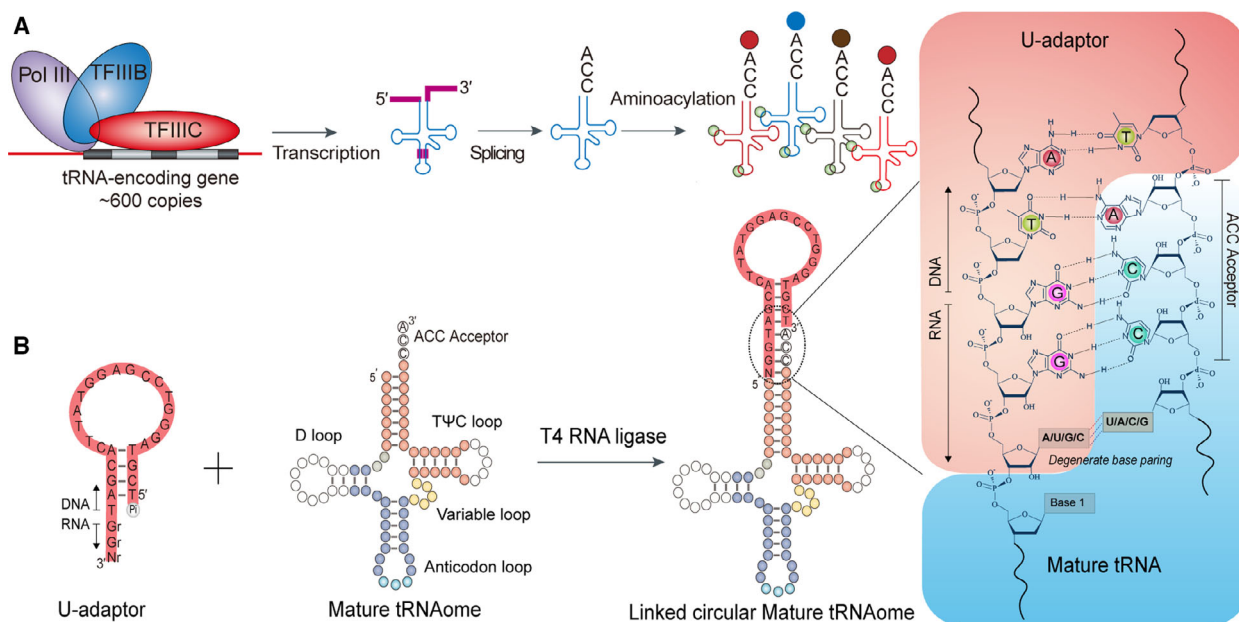


Fig. 2. A U-adaptor that interacts specifically with all mature tRNAs. (A) More than 600 tRNA-encoding genes can be transcribed by RNA polymerase III. After post-transcriptional processing, splicing and adding of ACC acceptor to these new tRNA transcripts are performed. The resulting mature tRNAome is available for all cellular mRNA translation and also for viral RNA decoding. The final step in tRNA maturation is adding the CCA sequence to which the acylating amino acid is coupled. The CCA tail is thus common and specific to all mature tRNAs. (B) A universal (U) DNA/RNA hybrid adaptor was designed. The -2 to -4 of 3'-terminal bases (TGG) of the U-adaptor are specifically designed to pair CCA acceptor. To further improve the compatibility of U-adaptor to all mature tRNAs, the last 3'-terminal nucleotide was degenerately designed. The interface of U-adaptor and mature tRNA is detailed at the right of the panel.

other tRNA species were downregulated following HEV infection. tRNA-Leu-UAG is most prominently downregulated by approximately 70%. We conclude that HEV infection provokes major remodeling of the mature tRNAome in cells capable of sustaining its replication.

HEV infection-triggered tRNAome remodeling is largely dependent on ORF2

The capsid protein of HEV encoded by ORF2 features many β -sheets in its secondary structure [28] and consequently requires incorporation of a multitude of proline and glycine residues during synthesis. By far, the most prominent effects of HEV infection on the tRNAome are the upregulation of tRNAs supporting proline and glycine decoding (tRNA-Pro-GGG, tRNA-Pro-UGG, and tRNA-Gly-CCC). Thus, we investigated the role of ORF2 in HEV-induced tRNA remodeling. We quantified tRNAome in cells carrying subgenomic HEV replicon with ORF2 deletion. This subgenomic HEV replicon contains a luciferase reporter, and viral replication can be quantified by luciferase activity (Fig. 4A). Intriguingly, although effects on tRNAome composition were still observed in the

subgenomic replicon (Fig. S6B), they are much moderate as compared to those in the full-length HEV model (Fig. S6C). Effects on tRNA-Pro-GGG, tRNA-Pro-UGG, and tRNA-Gly-CCC levels were not statistically significant in the subgenomic replicon.

Further insight came from unsupervised clustering analysis of the tRNAome profiles [29]. Three biologically independent experiments were performed with naïve Huh7 cells, Huh7 cells infected by HEV with the full-length genome, and cells carrying the subgenomic replicon. The experimental conditions segregated the profiles generated. As expected, the effects on tRNAome provoked by infection of HEV with full-length genome were much more pronounced as compared to those evoked by the subgenomic replicon (Fig. 4B). We, thus, conclude that ORF2 is essential for HEV-triggered tRNA remodeling.

HEV-induced tRNA remodeling may counteract decoding of interferon-stimulated genes

Innate antiviral immunity, especially that mediated by the so-called ISGs, is important for controlling HEV infection [30]. Interestingly, tRNAome remodeling by HEV mainly supported better decoding of ORF2 when

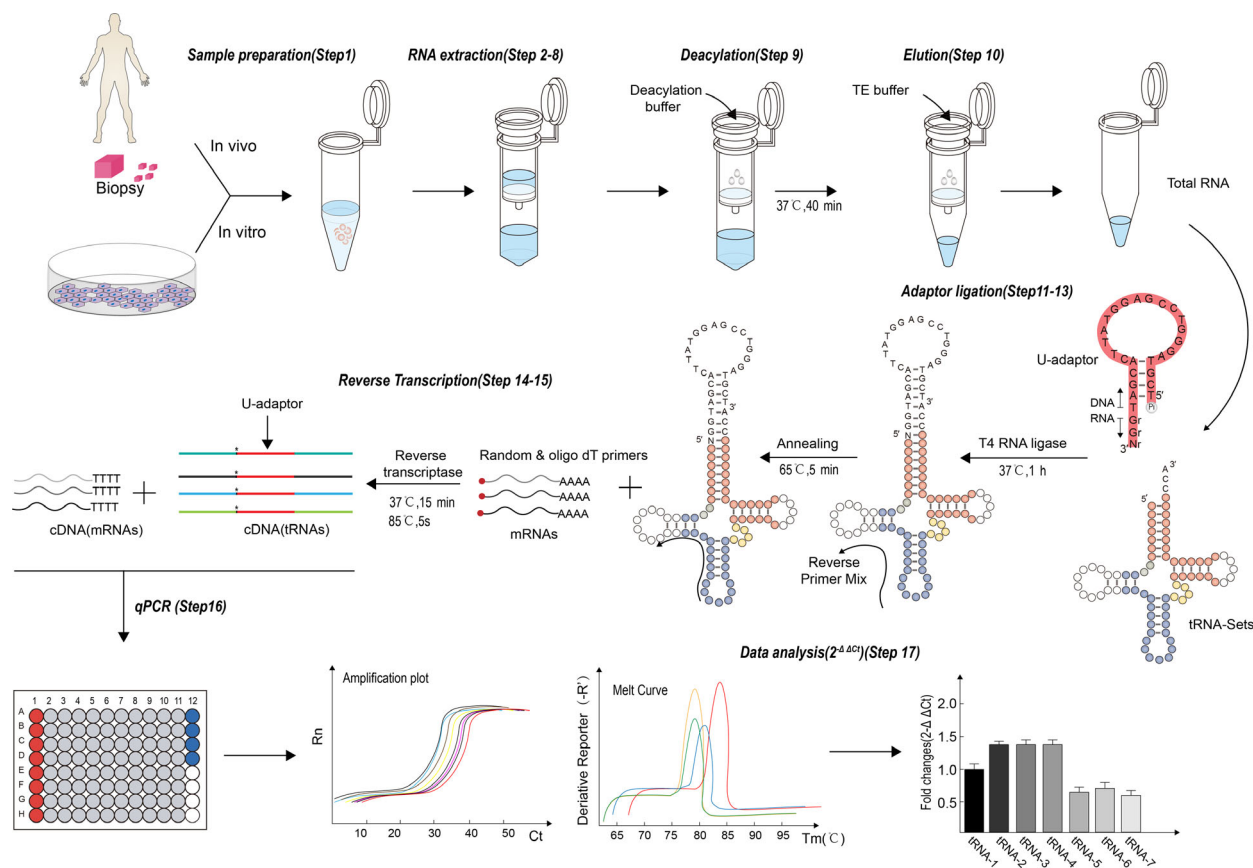


Fig. 3. Workflow of quantifying tRNAome. First, total RNA was extracted from the experimental systems involved according to a routine column-based RNA isolation protocol. Before elution, the column is incubated with deacylation buffer at 37 °C for 40 min to remove acylating amino acids at tRNA CCA tail followed by elution with TE buffer. Subsequently, the tRNA and U-adaptor are linked by T4 RNA ligase followed by annealing with reverse primer mix. Finally, the cDNA of total mRNA and U-adaptor-linked tRNAs are concurrently synthesized for qPCR amplification. The relative expression of tRNAs is calculated by $2^{-\Delta\Delta C_t}$ method that can be normalized by housekeeping genes, such as GAPDH. The stepwise procedures are detailed by seventeen discrete steps in [Materials and methods](#).

compared to ORF1 and ORF3 (Fig. 4C,D). Hence, we analyzed the effects of tRNAome remodeling triggered by full-length infectious HEV on the decoding of essential ISGs. We selected a panel of ISGs known to inhibit HEV infection. We found that HEV-provoked tRNA remodeling is not correlated with the RSCU of these ISGs (Fig. 4C and Table S5), whereas viral ORF2 translation *per se* is related to the same changes (Fig. 4C,D). We, thus, conclude that HEV infection reprograms the cellular tRNAome, which is likely to facilitate viral translation but hamper cellular antiviral immunity.

Discussion

The development of tRNA quantification methods has been greatly facilitated by the tRNAscan-SE program that allows accurate identification of genomic tRNA

sequences. Earlier methods to detect tRNAs usually involve thin-layer chromatography [31], liquid chromatography–mass spectrometry [32], DNA arraying [33], and single tRNA-based qPCR [15]. Recently, quantification of the tRNAome at transcriptional level has become more efficient through high-throughput sequencing [14,34], but is dependent on programming and very specific reagents. In this study, we established a simplified qPCR method for rapid quantification of the mature tRNAome. This strategy is characterized by a length-extension step, a universally compatible adaptor and degenerate primers applicable for the entire mature tRNAome. The present study was only demonstrated in a human cell model, but we envision that it is applicable to other organisms by adjusting primer design.

As a proof of principle, this qPCR methodology was used for characterizing the effects of HEV

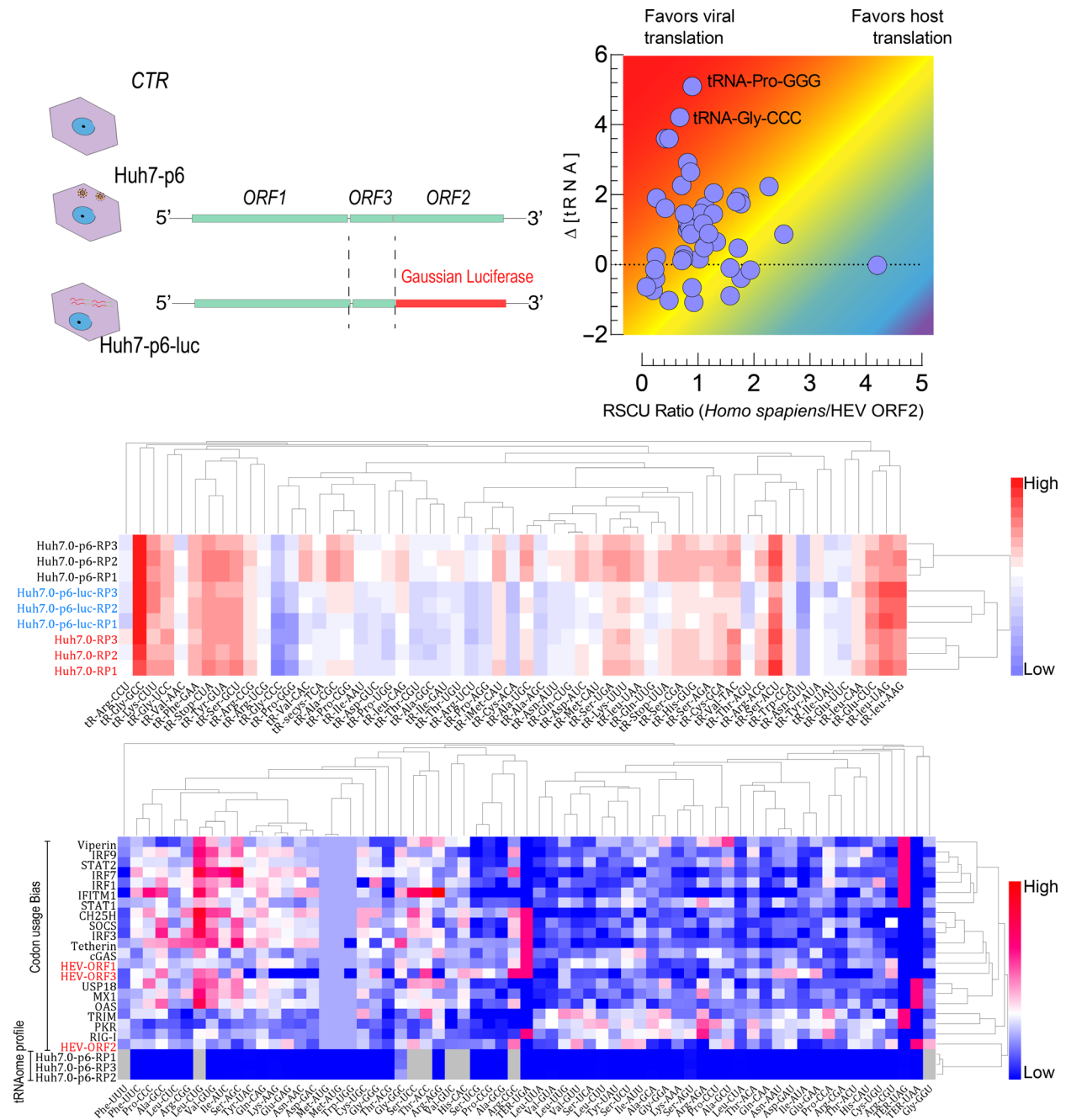


Fig. 4. tRNAome remodeling following HEV infection favors viral translation. (A) For profiling tRNAome, human hepatoma Huh7 cells harboring the infectious HEV clone with full-length genome (Huh7-p6), the subgenomic replicon lacking of ORF2 (Huh7-p6-luc), and naïve Huh7 cells were used ($n = 3$). (B) Cluster analysis of the tRNAome profiles in the three cell models. (C) Comparative analysis of the effects of HEV-induced tRNAome remodeling on codon usage of viral ORF (1–3) and a panel of antiviral ISGs. (D) Visualization of the effects of HEV infection on relative tRNA abundance in relation to viral and host codon decoding. For each tRNA, the ratio of HEV codon usage to human codon usage is plotted on the x-axis. A larger value indicates that a tRNA is more often used for human decoding as compared to viral decoding. The effect of HEV infection on tRNA abundance is plotted on the y-axis. A positive value corresponds to the upregulation of a tRNA following HEV infection.

infection on host tRNA^{ome}. We observed substantial remodeling of tRNA composition following HEV infection. For example, the level of tRNA-Pro-GGG was increased by 162 times by HEV infection. Such regulations appear in a fashion that facilitates translation of viral proteins while simultaneously hampering the decoding of antiviral ISGs. Interestingly, these observed effects relate especially to HEV ORF2, which is the dominant ORF of this virus with respect to demands on the host translational machinery [35]. Our data suggest that counteracting HEV-dependent tRNA remodeling may constitute a novel avenue for supporting host defense in combating viral infection, but this will require further understanding of the molecular pathways involved.

It has been reported that codon usage bias of the zoonotic genotypes 3 and 4 of HEV is much weaker than that of the nonzoonotic genotype 1 [19]. This indicates that less bias of HEV codon usage may be involved in zoonotic infection. Consistently, we found that genotype 3 HEV has not adapted its codon usage to that of its human host. This suggests that an alternative pathway may be used by HEV to facilitate cross-species infection, such as remodeling of tRNA^{ome}. It is well known that viral infection can hijack host cell physiology for weakening host defense and facilitating viral protein synthesis, which is dependent on the cellular mature tRNA^{ome}.

Recent studies have indicated that tRNA^{ome} disturbance has broad implications in many diseases, especially in cancer development and metastasis [23,36]. Further understanding of the role of tRNAs in biology and pathogenesis requires easy techniques to detect and quantify these molecules. In this respect, the U-adaptor strategy explored in the present study may provide new impetus and may form the basis for novel diagnostic possibilities. Hence, we envision that a convenient method, as the one presented in the current study, may prove instrumental for many aspects of contemporary biomedical research and practice with respect to tRNA biology.

Acknowledgements

This research was supported by the National Key Research and Development Program of China (2017YFD0500800), China Agricultural Research System (CARS-42-17), Science and Technology Program of Sichuan Province (20YYJC4428), and China Scholarship Council (Joint-Ph.D. fellowships 201706910003 to XO; Ph.D. fellowship 201508330291 to BM; and Ph.D. fellowship 201808530490 to RZ).

Author contributions

XO, AC, MP and QP designed the study and wrote the manuscript. BM, RZ, ZM, XO and QP did the experiments and analyzed the data. XO and BM analyzed the whole genomic tRNA data. XO, BM, MP, and QP generated the adaptor, primers and the qPCR pipeline. XO and RZ, performed the demonstration of tRNA^{ome} response upon viral infection.

References

- 1 Stern-Ginossar N and Ingolia NT (2015) Ribosome profiling as a tool to decipher viral complexity. *Annu Rev Virol* **2**, 335–349.
- 2 Novoa EM, Pavon-Eternod M, Pan T and de Poupiana LR (2012) A role for tRNA modifications in genome structure and codon usage. *Cell* **149**, 202–213.
- 3 Ou XM, Cao JY, Cheng AC, Peppelenbosch MP and Pan QW (2019) Errors in translational decoding: tRNA wobbling or misincorporation? *Plos Genet* **15**, e1008017.
- 4 Coleman JR, Papamichail D, Skiena S, Futcher B, Wimmer E and Mueller S (2008) Virus attenuation by genome-scale changes in codon pair bias. *Science* **320**, 1784–1787.
- 5 Lauring AS, Acevedo A, Cooper SB and Andino R (2012) Codon usage determines the mutational robustness, evolutionary capacity, and virulence of an RNA virus. *Cell Host Microbe* **12**, 623–632.
- 6 Shen SH, Stauff CB, Gorbatshevych O, Song Y, Ward CB, Yurovsky A, Mueller S, Futcher B and Wimmer E (2015) Large-scale recoding of an arbovirus genome to rebalance its insect versus mammalian preference. *Proc Natl Acad Sci USA* **112**, 4749–4754.
- 7 Eschke K, Trimpert J, Osterrieder N and Kunec D (2018) Attenuation of a very virulent Marek's disease herpesvirus (MDV) by codon pair bias deoptimization. *PloS Pathog* **14**, e1006857.
- 8 Li Y, Qu C, Yu P, Ou X, Pan Q and Wang W (2019) The interplay between host innate immunity and hepatitis E virus. *Viruses* **11**, 541.
- 9 Li M, Kao E, Gao X, Sandig H, Limmer K, Pavon-Eternod M, Jones TE, Landry S, Pan T, Weitzman MD *et al.* (2012) Codon-usage-based inhibition of HIV protein synthesis by human schlafen 11. *Nature* **491**, 125–145.
- 10 Smith BL, Chen GF, Wilke CO and Krug RM (2018) Avian influenza virus PB1 gene in H3N2 viruses evolved in humans to reduce interferon inhibition by skewing codon usage toward interferon-altered tRNA pools. *mBio* **9**, e01222-18.
- 11 Crick FH (1958) On protein synthesis. *Symp Soc Exp Biol* **12**, 138–163.
- 12 Chan PP and Lowe TM (2016) GtRNAdb 2.0: an expanded database of transfer RNA genes identified in

- complete and draft genomes. *Nucleic Acids Res* **44**, 184–189.
- 13 Kuhn CD, Wilusz JE, Zheng YX, Beal PA and Joshua-Tor L (2015) On-enzyme refolding permits small RNA and tRNA surveillance by the CCA-adding enzyme. *Cell* **160**, 644–658.
 - 14 Zheng GQ, Qin YD, Clark WC, Dai Q, Yi CQ, He C, Lambowitz AM and Pan T (2015) Efficient and quantitative high-throughput tRNA sequencing. *Nat Methods* **12**, 835–837.
 - 15 Honda S, Shigematsu M, Morichika K, Telonis AG and Kirino Y (2015) Four-leaf clover qRT-PCR: a convenient method for selective quantification of mature tRNA. *RNA Biol* **12**, 501–508.
 - 16 Kamar N, Izopet J, Pavio N, Aggarwal R, Labrique A, Wedemeyer H and Dalton HR (2017) Hepatitis E virus infection. *Nat Rev Dis Primers* **3**, 17086.
 - 17 Nimgaonkar I, Ding Q, Schwartz RE and Ploss A (2018) Hepatitis E virus: advances and challenges. *Nat Rev Gastroenterol Hepatol* **15**, 96–110.
 - 18 Meng XJ (2016) Expanding host range and cross-species infection of hepatitis E virus. *PLoS Pathog* **12**, e1005695.
 - 19 Zhou J-H, Li X-R, Lan X, Han S-Y, Wang Y-N, Hu Y and Pan Q (2019) The genetic divergences of codon usage shed new lights on transmission of hepatitis E virus from swine to human. *Infect Genet Evol* **68**, 23–29.
 - 20 Shukla P, Nguyen HT, Torian U, Engle RE, Faulk K, Dalton HR, Bendall RP, Keane FE, Purcell RH and Emerson SU (2011) Cross-species infections of cultured cells by hepatitis E virus and discovery of an infectious virus-host recombinant. *Proc Natl Acad Sci USA* **108**, 2438–2443.
 - 21 Shukla P, Nguyen HT, Faulk K, Mather K, Torian U, Engle RE and Emerson SU (2012) Adaptation of a genotype 3 hepatitis E virus to efficient growth in cell culture depends on an inserted human gene segment acquired by recombination. *J Virol* **86**, 5697–5707.
 - 22 Zhou XY, Wang YJ, Metselaar HJ, Janssen HLA, Peppelenbosch MP and Pan QW (2014) Rapamycin and everolimus facilitate hepatitis E virus replication: revealing a basal defense mechanism of PI3K-PKB-mTOR pathway. *J Hepatol* **61**, 746–754.
 - 23 Goodarzi H, Nguyen HCB, Zhang S, Dill BD, Molina H and Tavazoie SF (2016) Modulated expression of specific tRNAs drives gene expression and cancer progression. *Cell* **165**, 1416–1427.
 - 24 Gamble CE, Brule CE, Dean KM, Fields S and Grayhack EJ (2016) Adjacent codons act in concert to modulate translation efficiency in yeast. *Cell* **166**, 679–690.
 - 25 Coghlan A and Wolfe KH (2000) Relationship of codon bias to mRNA concentration and protein length in *Saccharomyces cerevisiae*. *Yeast* **16**, 1131–1145.
 - 26 van de Moosdijk AAA and van Amerongen R (2016) Identification of reliable reference genes for qRT-PCR studies of the developing mouse mammary gland. *Sci Rep* **6**, 35595.
 - 27 Berkhout B and van Hemert F (2015) On the biased nucleotide composition of the human coronavirus RNA genome. *Virus Res* **202**, 41–47.
 - 28 Guu TSY, Liu Z, Ye QZ, Mata DA, Li KP, Yin CC, Zhang JQ and Tao YJ (2009) Structure of the hepatitis E virus-like particle suggests mechanisms for virus assembly and receptor binding. *Proc Natl Acad Sci USA* **106**, 12992–12997.
 - 29 Johnson SC (1967) Hierarchical clustering schemes. *Psychometrika* **32**, 241–254.
 - 30 Wang W, Wang Y, Qu C, Wang S, Zhou J, Cao W, Xu L, Ma B, Hakim MS, Yin Y *et al.* (2018) The RNA genome of hepatitis E virus robustly triggers an antiviral interferon response. *Hepatology* **67**, 2096–2112.
 - 31 Spears JL, Gaston KW and Alfonzo JD (2011) Analysis of tRNA editing in native and synthetic substrates. In *RNA and DNA Editing*, pp. 209–226. Springer, Berlin.
 - 32 Gaston KW and Limbach PA (2014) The identification and characterization of non-coding and coding RNAs and their modified nucleosides by mass spectrometry. *RNA Biol* **11**, 1568–1585.
 - 33 Grelet S, McShane A, Hok E, Tomberlin J, Howe PH and Geslain R (2017) SPOT: A novel and streamlined microarray platform for observing cellular tRNA levels. *PLoS One* **12**, e0177939.
 - 34 Schwartz MH, Wang H, Pan JN, Clark WC, Cui S, Eckwahl MJ, Pan DW, Parisien M, Owens SM, Cheng BL *et al.* (2018) Microbiome characterization by high-throughput transfer RNA sequencing and modification analysis. *Nat Commun* **9**, 5355.
 - 35 Ankavay M, Montpellier C, Sayed IM, Saliou J-M, Wychowski C, Saas L, Duvet S, Aliouat-Denis C-M, Farhat R, de Masson d'Autume V *et al.* (2019) New insights into the ORF2 capsid protein, a key player of the hepatitis E virus lifecycle. *Sci Rep* **9**, 6243.
 - 36 Grewal SS (2015) Why should cancer biologists care about tRNAs? tRNA synthesis, mRNA translation and the control of growth. *Biochim Biophys Acta* **1849**, 898–907.

Supporting information

Additional supporting information may be found online in the Supporting Information section at the end of the article.

Fig. S1. Comparative analysis of codon usage bias of HEV isolated from monkey and human.

Fig. S2. Usefulness of U-adaptor to detect 57 types of tRNA sets in human genome.

Fig. S3. Melt curves and variation analysis of 57 tRNA types.

Fig. S4. Specific and quantifiable expression of tRNAs that can be related to HEV infection levels.

Fig. S5. Failed efforts aimed at protocol optimization.

Fig. S6. Relative transcription levels of 57 tRNA types following infection with either full length HEV or an ORF2-lacking subgenomic replicon.

Table S1. Key materials used in this study.

Table S2. Primers used in mature tRNAome detection.

Table S3. Preparation of qPCR mix.

Table S4. Specifics of the qPCR analysis.

Table S5. Interferon stimulated genes (ISGs) used in this study.